

Modeling nonlinearity and hysteresis due to critical-state flux penetration in hard superconductors

T. Dasgupta, Durga P. Choudhury and S. Sridhar

Department of Physics, Northeastern University, Boston, MA 02115

Abstract— **The nonlinear surface impedance of a thin superconducting strip carrying a microwave current was calculated numerically from first principles based upon flux penetration due to a current-induced critical state. Our results approaches the analytical results in the appropriate limit. The technique is useful for design of passive superconducting microwave circuits.**

Keywords— **Critical state, Hysteresis, Nonlinearity, Microwave Transmission Lines**

I. INTRODUCTION

SINCE its discovery, the new breed of oxide superconductors with transition temperatures above the boiling point of nitrogen have shown great potential as a replacement for metals for passive microwave structures owing to their very low surface resistance[1], [2], [3]. However, a key feature of the high temperature superconductivity is the inherently nonlinear response at microwave frequencies, which is present over a wide range of input powers. This nonlinear responses also poses a major challenge for numerical device design using these materials. Most existing computer aided design software do not take into account the inherent nonlinearity of superconductors. The few analytical models that do exist[4] are valid only for highly idealized geometries and need to be incorporated into practical device design.

There are several physical models of nonlinear surface resistance, each valid in a different regime of temperature and microwave power[5]. The most popular models are pinning induced critical state[4], [6], [7], transport current induced self-heating [8], and depairing [8]. The current-driven critical state model [4] has proven to be particularly useful not only because it fits experimental measurement of R_S very accurately over a wide range of temperature and power levels [9], but also because its usefulness extends to modeling hysteretic losses in superconducting transmission lines.

The (field-induced) critical state model was first proposed by Bean[10] to explain the unusual magnetization behavior of hard superconductors and was first solved for the geometry of a semi-infinite slab where the field was applied parallel to its face. The geometry where the field is applied perpendicular to a thin strip was solved relatively recently by several groups and the field and current distribution[11], [12] and the surface impedance from hysteretic loss[4] was obtained analytically.

Though very elegant, the analytic results were restricted

to certain “ideal” geometries only where symmetry could be used to simplify the problems. However, these idealizations are not always satisfied in real world applications of superconducting strips in microwave circuits. In the wake of the fact that the model does describe experimental data accurately [9], it is imperative to be able to implement a numerical paradigm without the constraints of the idealized geometry required by the analytic approach.

In this paper, we demonstrate a numerical approach to incorporate the nonlinear response of superconducting materials using assumptions equivalent to those of the current induced critical state.

II. THE CRITICAL STATE MODEL

Let us consider a infinitely long stripline of width $2a$ and thickness δ carrying a total current $I = I_0 \cos(\omega t)$. The geometry of the center conductor and our choice of axes is shown in of Fig.1. For simplicity we shall assume that the frequency ω of the applied transport current is low enough, so that the problem can be dealt in a quasi-static way and that the ground planes are far away from the central superconductor, so that it carries a negligible current and hence does not effect the magnetic field distribution inside the center conductor[13].

We start with the most generic physical assumptions that retain the essential ideas of critical states:

The current density inside the central conductor $\mathbf{j}(\mathbf{r}) = j(y)\hat{\mathbf{k}}$ (where $\hat{\mathbf{k}}$ is a unit vector along the z -direction) is such that,

1. $|j(x, y)| \leq j_c$ and $|j(|y| > b)| = j_c$ where j_c is the critical current density.
2. The magnetic induction $\mathbf{B}(x, y) = 0$ for $|y| \leq b \leq a$

The first assumption highlights the fact that flux lines are pinned until the Lorenz force on them exceeds a certain critical value. The second assumption follows from the fact that the vortices start penetrating from the edges. Hence for any given current there would be a flux free region in the center of the strip. Also note that the depinning critical current is at least an order of magnitude smaller than the depairing critical current where superconductivity would be quenched by the self field.

In the following we show that for a strip with finite thickness, this model can be solved numerically and that it leads to unique field and current distribution within the strip. We further show that (1) and (2) leads to hysteresis irrespective of the geometry and study the hysteresis laws for the

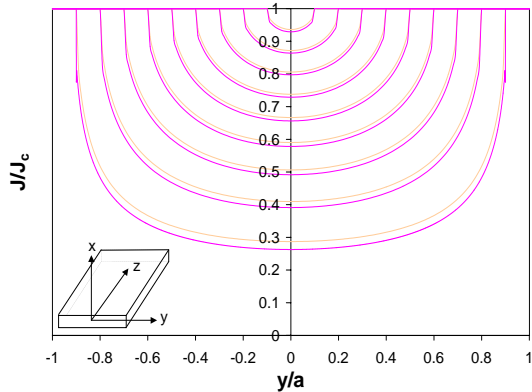


Fig. 1. Current distribution j/j_c across the strip for $b/a = 0.1, 0.2, \dots, 0.9$. The lower (solid) lines are numerical calculations and the upper (dashed) lines are analytic calculations[12]. The inset shows the geometry and our choice of axes. The length of the strip (and the current) is along the z -direction and the width is along the y -direction such that the centre of the strip is at the origin.

specific strip geometry under consideration.

III. COMPUTATIONAL DETAILS

A semi-numerical approach was used to determine a current distribution which satisfies the two assumptions presented above. Assuming an uniform current distribution along the x -direction one can show that

$$B(x=0, y) = \frac{\mu_0}{\pi} \int_{-a}^a j(y') \tan^{-1} \left[\frac{\delta}{2(y-y')} \right] dy' \quad (1)$$

The above analytical expression for $B(x=0, y)$ in eq(1) was used to save computational time.

In the model which requires that $j(y : b \leq |y| \leq a) \equiv j_c$ and $B(x=0, |y| \leq b < a) = 0$, one needs to solve for the current distribution in the field free region $|y| \leq b < a$

$$\int_{-a}^a j(y') \tan^{-1} \left[\frac{\delta}{2(y-y')} \right] dy' = 0 \text{ for } |y| \leq b < a \quad (2)$$

Numerical solutions of integral equations such as eq(2) are rather complicated. We found a simpler iterative approach to find the current density in the field free region of the superconducting strip. Here we give a brief description of the algorithm that was used.

Suppose that the thickness of the strip is infinite ($\delta \rightarrow \infty$). Then for any given initial current distribution $j(y)$, a field free region $B(|y| \leq b) \equiv 0$ can be obtained by replacing the current density in that region with

$$j(|y| < b) \rightarrow j(|y|) + \frac{\partial}{\partial y} B_x \quad (3)$$

Also note that the magnetic field strength on the line $x=0$ for a slab ($\delta \rightarrow \infty$) is mostly effected by the current on and around the line $x=0$. Therefore, for the case of a finite δ , the transformation in eq(3) will bring the field

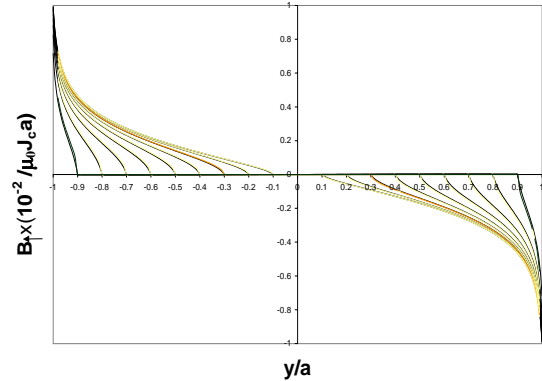


Fig. 2. The magnetic field strength $B(x=0, y/a)$ across the strip for $I/I_{\max} = 0.41, 0.58, 0.70, 0.79, 0.86, 0.91, 0.95, 0.98, 0.99$.

strength in the region $|y| < b$ a little closer to zero. Hence an iterative implementation of the above transformation of $j(y)$ in eq(3) will eventually converge, bringing the magnetic field strength in the region $|y| < b$ to zero, irrespective of the size of δ .

In a nutshell, we start with a flat current distribution, $j(y) = j_c$ in an one dimensional grid of size 4000 and we iteratively make $B(x=0, |y| < b)$ vanish by replacing the current density by $j_y^{n+1} \rightarrow j_y^n + (B_{y+1}^n - B_y^n) / \Delta y$ at every step.

IV. RESULTS

We first discuss the current and the field profiles inside the central conductor. In our analysis, we chose $\delta/2a = 0.01$. In Fig.1 we present the current profile inside the strip in this model for $b/a = 0.1$ to 0.9 . For the purpose of comparison, we also plot the analytical results in the $\delta \rightarrow 0$ limit (dashed lines). As one can see, the current density in the flux free region for the strip of finite thickness is lower. This is expected, since for the slab geometry, $\delta \rightarrow \infty$, where again one can solve the problem analytically, the current density in the field free region is zero. In Fig.2 we plot the corresponding magnetic field distributions. In Fig.3(a and b) we plot a 3-D and contour plot respectively of the magnetic field strength for a sample value of $b/a = 0.7$. The contour diagram in Fig.3b, displays the field lines in and around the magnetic strip. The dotted rectangle shows the perimeter of the cross-section of the stripline. As one can see from the field lines inside the conductor, the fields are almost entirely in the y -direction. Note that the darker contour lines represents smaller field strength, hence the field strength inside the “flux free region” of the conductor is relatively small compared to the field strength in the entire region displayed in the plot.

A. Hysteresis

The hysteresis law can be derived by studying the current density distribution for an oscillating current over a full cycle. If the current density distribution for a total current

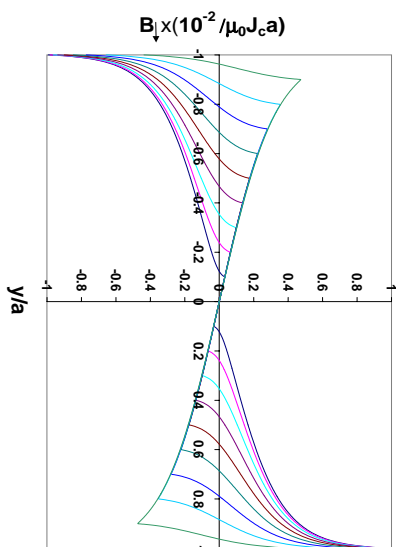
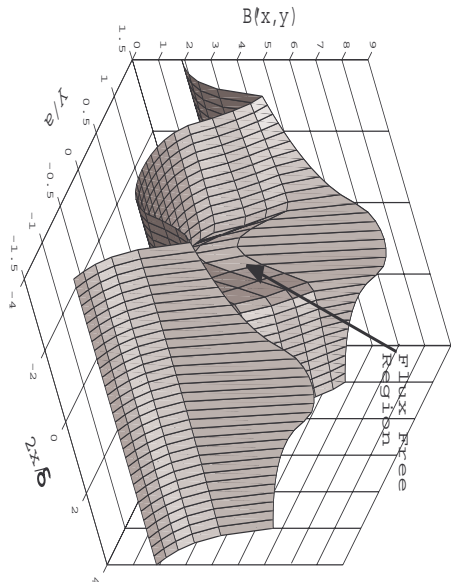


Fig. 4. Magnetic field strength, $B(x = 0, y/a)$, when I is reduced from $I_0 = I_{max} = 2j_c\delta a$ to $-I_{max}$. This graph displays the origin of hysteresis. We plot B across the strip for $I/I_{max} = 0.18, -0.17, -0.40, -0.58, -0.72, -0.82, -0.90, -0.96, -0.99$.

$-2j_c\delta a$. As evident from the figure, we no longer see any flux free region inside the strip, even when the transport current $I = 0$. In other words, once exposed to a current of $2j_c\delta a$, there will no longer be a flux free region inside the strip, irrespective of the transport current. This sort of phenomenon is unique to hysteresis.

B. Penetration Law

We calculate the flux penetration depth d/a for the strip as a function of the peak transport current. In Fig.5 we display $b/a = (1 - d/a)$ as a function of the peak transport current I_0/I_{max} and compare that with the analytical results for a strip of zero thickness[12]. Here I_{max} is the maximum transport current and is given by $I_{max} = 2a\delta j_c$.

As one can see from Fig.1 and Fig.5 that the penetration law gets more linear and the current density in the field free region decreases as we go from zero thickness to a finite thickness. This is expected, since in the limit $\delta \rightarrow \infty$ we expect a linear penetration law and $j(x = 0, |y| \leq b < a) = 0$. These results along with the steady state current and field profiles can then determine the current critical states and the corresponding magnetic field distribution for alternating currents.

C. Surface Impedance

Assuming that the strip is excited with a current of amplitude I_0 and frequency $\omega = \frac{2\pi}{T}$, the electric field $E_z(y, t)$ along the line $x = 0$ is be given by

$$E_z(y, x, t) = -\frac{d}{dt} \int_0^y dy' B_x(y', x, t) \quad (7)$$

and the energy lost per unit length of the strip in a half cycle is

$$U_{H.C.} = 2 \int_{-\frac{\delta}{2}}^{\frac{\delta}{2}} dx \int_0^a dy \int_{-T/4}^{T/4} dt j_z(y, t) E_z(y, x, t) \quad (8)$$

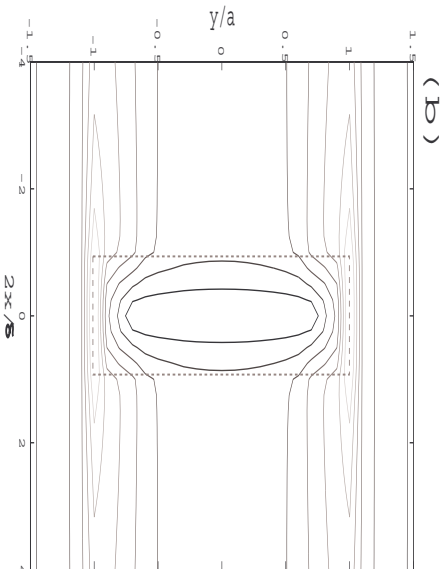


Fig. 3. The magnetic field strength $B(x, y) (= B(x, y)/(100\mu_0 j_c a)$: (a) 3-D and (b) contour graph displaying the field free region for $b/a = 0.7$. In (b) the lighter the contour the stronger the fields. The dark elliptical curves inside the dotted rectangle (the cross-section of the stripline) represents the field lines of the extremely weak fields inside the superconductor.

I is $j(y, I, j_c \rightarrow \infty)$, then in the case of an infinite critical current, the current density will be $Nj(y, I, j_c \rightarrow \infty)$ for a total current of NI . In other words

$$j(y, NI, j_c \rightarrow \infty) = Nj(y, I, j_c \rightarrow \infty) \quad (4)$$

However, since $j(y) \leq j_c$ everywhere, the current density distribution depends on the total current. That is

$$j(y, NI, j_c) \neq Nj(y, I, j_c). \quad (5)$$

When the current is reversed after reaching its peak value I_0 , the current density starts to decrease from the edges with an *effective* critical current density of $2j_c$ in the opposite direction . This is because, at $I = I_0$ the current density at the edges is j_c in the positive z -direction. Thus the hysteresis law on the downward cycle is given by[12]

$$j_{\downarrow}(y, I, j_c) = j_{max}(y, I_0, j_c) - j_{\uparrow}(y, I_0 - I, 2j_c) \quad (6)$$

Fig. 4 displays the magnetic field distribution when the input current is reduced from the maximum current $2j_c\delta a$ to

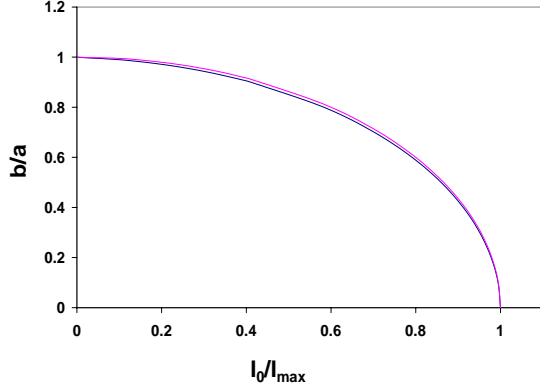


Fig. 5. Penetration Law: $b = (1 - d/a)$ as a function of peak current I_0/I_{max} . The upper curve represents the analytical results for zero thickness[12] and the lower one represents the numerical results for a finite strip.

Substituting eq(7) and integrating by parts we get

$$\begin{aligned}
 U_{H.C.} &= -2 \int_{-\frac{\delta}{2}}^{\frac{\delta}{2}} dx \int_0^a dy \int_{-T/4}^{T/4} dt j_c \times \\
 &\quad \frac{d}{dt} \int_{b(I_0)}^y dy' B_x(y', x, t) \\
 &= -4j_c \int_{-\frac{\delta}{2}}^{\frac{\delta}{2}} dx \int_{b(I_0)}^a dy \int_{b(I_0)}^y dy' B_x(y', x, 0)
 \end{aligned} \quad (9)$$

This definition of $U_{H.C.}$ was also used by Brandt in ref.[12]. This defines the resistance per unit length of the stripline as

$$\begin{aligned}
 R' &= \frac{R}{l} = \left(\frac{\mu_0}{4T \times 10^{-4}} \right) \times 2 \frac{4j_c}{(I_0^2/I_{max}^2)} \int_{-\frac{\delta}{2}}^{\frac{\delta}{2}} d\left(\frac{x}{\delta}\right) \times \\
 &\quad \int_{\frac{b(x_0)}{a}}^1 d\left(\frac{y}{a}\right) \int_{\frac{b(x_0)}{a}}^{\frac{y}{a}} d\left(\frac{y'}{a}\right) \left(\frac{B_x(y'/a, x/\delta, 0)}{10^2 \mu_0 j_c a} \right)
 \end{aligned} \quad (11)$$

where l is the length of the strip. Fig.6 displays the resistance R' per unit length as a function of the peak current, I_0/I_{max} . For comparison purposes, we also plot the analytical results for R' [4]

$$\begin{aligned}
 R' &= \frac{p}{I_0^2/I_{max}^2} = \frac{I_{max}^2}{\pi I_0^2} \left\{ \left(1 - \frac{I_0}{I_{max}}\right) \ln \left(1 - \frac{I_0}{I_{max}}\right) \right. \\
 &\quad \left. + \left(1 + \frac{I_0}{I_{max}}\right) \ln \left(1 + \frac{I_0}{I_{max}}\right) - \left(\frac{I_0}{I_{max}}\right)^2 \right\}
 \end{aligned} \quad (12)$$

As one can see, the two plots almost falls on top of each other. This is expected, since our results for $j_z(y)$ and $B_x(y)$, are close to that of the strip of zero thickness.

Calculation of reactance in a nonlinear model like the one at hand are in general more involved. Here nonlinearity refers to the fact that, in this model a transport current of $I(t) = \text{Re}(I_0 e^{i\omega t})$ gives rise to a current density of

$$j(x, y, t) = \text{Re} \left(\sum_{n=0}^{\infty} j_n(x, y) e^{(2n+1)i\omega t} \right) \quad (13)$$

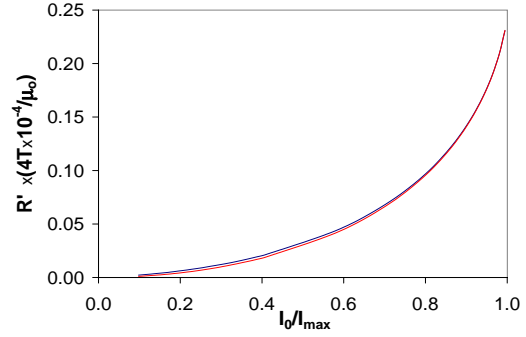


Fig. 6. Resistance per unit length, R' as a function of the peak current I_0/I_{max} . The upper curve displays our numerical results for a finite strip. The lower curve is a plot of the analytical expected value of R_s [4].

where in eq.(13), $j_n(x, y)$'s are complex. Note however that in terms of the Fourier components, the problem is harmonic, that is each of the harmonics $j_n(x, y)$ will uniquely determine the corresponding harmonics of the electric and magnetic field strength through the microscopic Maxwell's equations. Hence an exact calculation of the reactance will mean calculating the individual reactance for each of these harmonics and adding them up. Although this is possible, this is a rather big problem in itself. It can be shown however, that the total reactance per unit length of the stripline (neglecting the higher order effects) can be calculated with reasonable accuracy using

$$\begin{aligned}
 X' &= \frac{X}{l} \approx \frac{\omega}{\mu_0 I_0^2} \int_{-\infty}^{\infty} dy \int_{-\infty}^{\infty} dx B^2(x, y : I = I_0) \\
 &= \left(\frac{\mu_0 \pi}{2T \times 10^{-8}} \right) \frac{1}{\mu_0 (I_0^2/I_{max}^2)} \int_{-\infty}^{\infty} d\left(\frac{y}{a}\right) \times \\
 &\quad \int_{-\infty}^{\infty} d\left(\frac{x}{\delta}\right) B^2\left(\frac{x}{\delta}, \frac{y}{a} : I = I_0\right)
 \end{aligned} \quad (15)$$

We carry out the space integral until $B^2(x, y)$ falls down by 99% of its peak value. Fig.7 displays the reactance X' per unit length as a function of the peak current, I_0/I_{max} . Here again, we show that for small values of the current $X' \approx \left(\frac{I_0}{I_{max}}\right)^2$ which conforms the analytical results in ref. [4].

V. CONCLUSION

A first principle numerical calculation on a strip of finite thickness using assumptions similar to the critical state model yields results that approach the analytic results in the appropriate limits ($\delta \rightarrow 0$) but without the unrealistic idealizations of the later. Further a numerical approach gives one the flexibility of accommodating higher complexities like effects due to the ground planes and more accurate calculations of surface impedance and harmonics. This topic

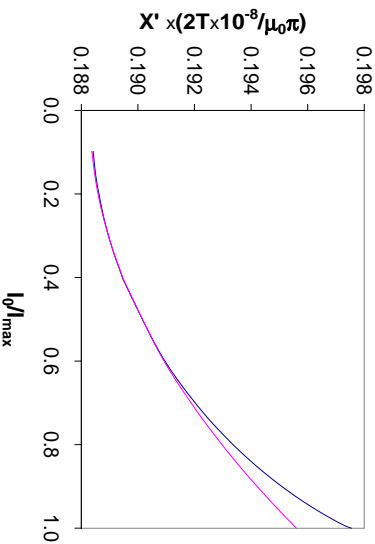


Fig. 7. Reactance per unit length, X' as a function of the peak current I_0/I_{max} . The upper curve represents our numerical results for the finite strip, and the lower curve is a quadratic fit confirming that, for low currents X_s is quadratic in current [4].

will be addressed in future work. This approach can be implemented into a computer aided design framework for the design of passive superconducting microwave components.

VI. ACKNOWLEDGMENTS

This work benefited from the allocation of time at the Northeastern University Advanced Scientific Computing Center (NU-ASCC). This work is supported by NSF-9711910 and AFOSR by F49620-98-1-0021.

REFERENCES

- [1] E. Zeldov, John R. Clem, M. M. McElfresh, and M. Darwin, "Magnetization and transport currents in thin superconducting films," *Phys. Rev. B*, vol. 49, no. 14, pp. 9802–9822, April 1994.
- [2] Ernst Helmut Brandt and Mikhail Indenbom, "Type-II superconductor strip with current in a perpendicular magnetic field," *Phys. Rev. B*, vol. 48, pp. 12893–12906, 1993.
- [3] A. M. Campbell, "," *IEEE Trans. Appl. Supercond.*, vol. 5, pp. 687, 1995.
- [1] Durga P. Choudhury and S. Sridhar, "Superconducting microwave technology," in *Wiley's Encyclopedia of Electrical and Electronic Engineering*, Vol. 21 pp. 28-39 John Wiley & Sons, New York, 1999.
- [2] M. J. Lancaster, *Passive microwave device applications of high temperature superconductors*, Cambridge University Press, New York, 1997.
- [3] Zhi-Yuan Shen, *High-Temperature Superconducting Microwave Circuits*, Artech House, Boston, 1994.
- [4] S. Sridhar, "Non-linear microwave impedance of superconductors and ac response of the critical state," *Appl. Phys. Lett.*, vol. 65, no. 8, pp. 1054–1056, August 1994.
- [5] M. A. Golosovsky, H. J. Shortland, and M. R. Beasley, "Nonlinear microwave properties of superconducting Nb microstrip resonators," *Phys. Rev. B*, vol. 51, no. 10, pp. 6462–6469, March 1995.
- [6] J. McDonald, John R. Clem, and D. E. Oates, "Critical-state model for harmonic generation in a superconducting microwave resonator," *Phys. Rev. B*, vol. 55, no. 17, pp. 11823–11831, May 1997.
- [7] J. McDonald, J. R. Clem, and D. E. Oates, "Critical-state model for intermodulation distortion in a superconducting microwave resonator," *J. Appl. Phys.*, vol. 83, no. 10, pp. 5307–5312, May 1998.
- [8] M. Golosovsky and M. Tsindlekt and H. Chayet and D. Davydov "Vortex depinning frequency in $YBa_2Cu_3O_{7-x}$ superconducting thin films — anisotropy and temperature dependence," *Phys. Rev. B*, vol. 50, no. 1, pp. 470, Jul 1994.
- [9] Balam A. Willmsen, John S. Derov, José H. Silva, and S. Sridhar, "Nonlinear response of suspended high temperature superconducting thin film microwave resonators," *IEEE Trans. Appl. Supercond.*, vol. 5, no. 2, pp. 1753–1755, June 1995.
- [10] C. P. Bean, "Magnetization of hard superconductors," *Phys. Rev. Lett.*, vol. 8, pp. 250–253, 1962.